Optical Fiber Technology 94 (2025) 104313

Contents lists available at ScienceDirect

Optical Fiber Technology

journal homepage: www.elsevier.com/locate/yofte

Single-polarization hollow-core anti-resonant fiber with ultra-high polarization loss ratio and low loss in the terahertz range

Qiang Liu [a,b], Xiaotian Yao [a,b], Jian Han [a,b], Guangrong Sun [c], Zihao Lan [a,b], Peiqing Xing [a,b], Jingwei Lv [a,b], Paul K. Chu [d], Chao Liu [a,b,*]

[a] SANYA Offshore Oil & Gas Research Institute, Northeast Petroleum University, Sanya 572024, China
[b] School of Physics and Electronic Engineering, Northeast Petroleum University, Daqing 163318, China
[c] College of Advanced Interdisciplinary Studies, National University of Defense Technology, Changsha 410073, China
[d] Department of Physics, Department of Materials Science and Engineering, and Department of Biomedical Engineering, City University of Hong Kong, Tat Chee Avenue, Kowloon, Hong Kong, China

ARTICLE INFO

Keywords:
Single-polarization filter
Hollow-core anti-resonant fiber
Double-layer nested elliptical tube
Theoretical simulation

ABSTRACT

A single-polarization hollow-core anti-resonant fiber (HC-ARF) with an asymmetric cladding and double-layer nested elliptical tube is designed and analyzed. Along the X-axis, the outer elliptic tube with gradually varying wall thickness and the inner elliptic tube with a uniform wall thickness enhance the loss of the X-polarized fundamental mode (FM). In the Y-axis direction, the double-layer elliptic tube with a uniform wall thickness suppresses the loss of Y-polarized FM to improve the polarization loss ratio (PLR). Theoretical analysis reveals that the losses of X-polarized FM and Y-polarized FM at 1 THz are 9.07 dB/m and 2.59×10^{-5} dB/m, respectively, and PLR is 349,318 and greater than 100 between 0.98 and 1.02 THz. The HC-ARF with properties better than similar filters reported recently is a new design for high-performance terahertz-band single-polarization fibers with great application potential.

1. Introduction

Terahertz waves have garnered interest in imaging [1], sensing [2], communication [3], security monitoring [4], medical examination [5], drug detection [6] and military applications [7]. Optical fibers play a significant role in terahertz wave transmission and sensing, especially hollow-core anti-resonant fibers (HC-ARFs) which have desirable properties such as low loss, low nonlinearity, small dispersion, and high damage thresholds [8]. HC-ARFs, which make use of the coherent reflection between tubular glass films of the fiber cladding to confine light to the air core, are used in high-power laser transmission [9,10], optical communication [11], optical fiber gyroscopes [12], pulse compression [13,14], and optical fiber sensing [15]. However, the transmission quality of optical signals must be improved to cater to commercial applications, and it is important to design single-polarization optical fibers that can control light polarization.

To design high-performance single-polarization fibers, two methods are commonly used. The first technique is to coat or fill the cladding tube in a certain direction with high refractive index materials [16] to enhance the coupling between the cladding mode and FM without affecting the other orthogonal direction. The second method is to adopt an asymmetric cladding structure [17], in which the cladding tube satisfies the resonance condition in one direction and enhances the FM loss of the polarized direction. The cladding tubes of the other orthogonal direction satisfy the antiresonance condition to confine the FM mode in the fiber core and reduce transmission losses. The properly designed single-polarization fiber can avoid polarization crosstalk and polarization mode dispersion caused by the fundamental mode in both polarization directions [18]. For example, S. Yan et al. [19] have proposed a single-mode, single-polarization fiber with six double-ring node-free structures with different wall thicknesses in the two orthogonal directions to achieve a polarization loss ratio (PLR) of 17,662 at 1,550 nm and two single-polarization transmission bands of 1,545–1,553 nm and 1,591–1,596 nm. S. Yan et al. [20] have reported a double-ring cladding in which the inner layer in the Y-axis direction is coated with a layer of high refractive index silicon to enhance the coupling between the Y-polarized FM and cladding mode, resulting in a PLR of 14,232 at 1,520 nm. Y. Gong et al. [21] have proposed an asymmetric five-tube nested double C-type structure, which breaks the axisymmetric distribution of refractive indexes by covering a layer of high-refractive-index silicon on

* Corresponding author at: SANYA Offshore Oil & Gas Research Institute, Northeast Petroleum University, Sanya 572024, China.
E-mail address: msm-liu@126.com (C. Liu).

https://doi.org/10.1016/j.yofte.2025.104313
Received 30 December 2024; Received in revised form 2 May 2025; Accepted 15 June 2025

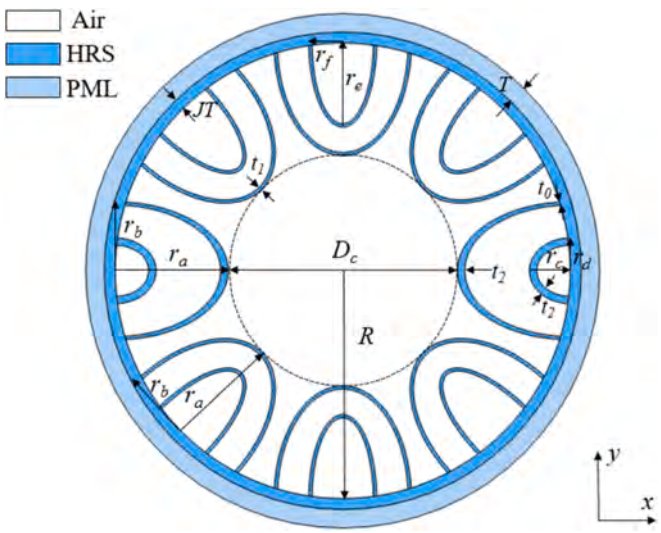

Fig. 1. Cross-sectional schematic of the HC-ARF.

the inner surface of the X-axis cladding tubes. The PLR is 162,486 at 1,550 nm, and the single-polarization bandwidth is 150 nm. However, in the terahertz band, the fiber absorbs terahertz waves more strongly, rendering it difficult to enhance the PLR. The single-polarization fiber reported by Ankan et al. [22] has a four-tube nested semi-elliptical structure with a single semi-elliptical tube in the Y-axis direction and a double semi-elliptical tube in the X-axis direction. The loss is 4.8 dB/m at 0.9 THz, and the PLR is 2.5. Mollah et al. [23] have reported a four-tube nested structure based on Zeonex showing a minimum loss of 0.34 dB/m and PLR of 13 at 1.1 THz. L. Xue et al. [24] have designed a terahertz HC-ARF with four tubes nested in a semi-elliptical tube. The X-axis cladding tubes have the resonant wall thickness, and the Y-axis cladding tubes have the anti-resonant wall thickness showing a PLR of 156 at 0.5 THz. Q. Liu et al. [25] have reported a polarization filter based on HC-ARF with a double-connected tube cladding structure, showing a polarization extinction ratio of 100 dB at 1 THz, and the insertion loss of Y-polarized FM at 1 THz is less than 0.66 dB. The existing single-polarization fibers are mostly made of polymer materials, such as Zeonox, TOPAS which have higher absorption coefficient of 0.276 cm^{-1} at 1THz [22,24]. The absorption and scattering losses of the polymer materials are large, which result in higher loss, lower PLR.

Herein, an asymmetric double-layer nested semi-elliptical tube HC-ARF is designed and analyzed. High-resistivity silicon (HRS) with lower absorption coefficient is used to form the fibers. The X-axis cladding has double-layer nested semi-elliptical tubes with gradually changing wall thickness on the outer tube and uniform wall thickness for the inner tube. In the structure showing enhanced X-polarized FM losses, the Y-axis double-layer nested semi-elliptical tubes with a uniform wall thickness reduce the Y-polarized FM loss to realize single-polarization and ultra-high PLR. The losses of X-polarized FM and Y-polarized FM at 1 THz are 9.07 dB/m and 2.59×10^{-5} dB/m, respectively. The PLR is 349,318, and the PLR is greater than 100 in the range of 0.98–1.02 THz. Our results reveal a novel strategy for designing terahertz polarization filters and polarization-maintaining fibers.

2. Structure

Fig. 1 shows the HC-ARF with the asymmetric double-layer nested elliptic tube. In the X-axis direction, the two double-layer semi-elliptical nesting structures with gradient wall thickness in the outer layer and

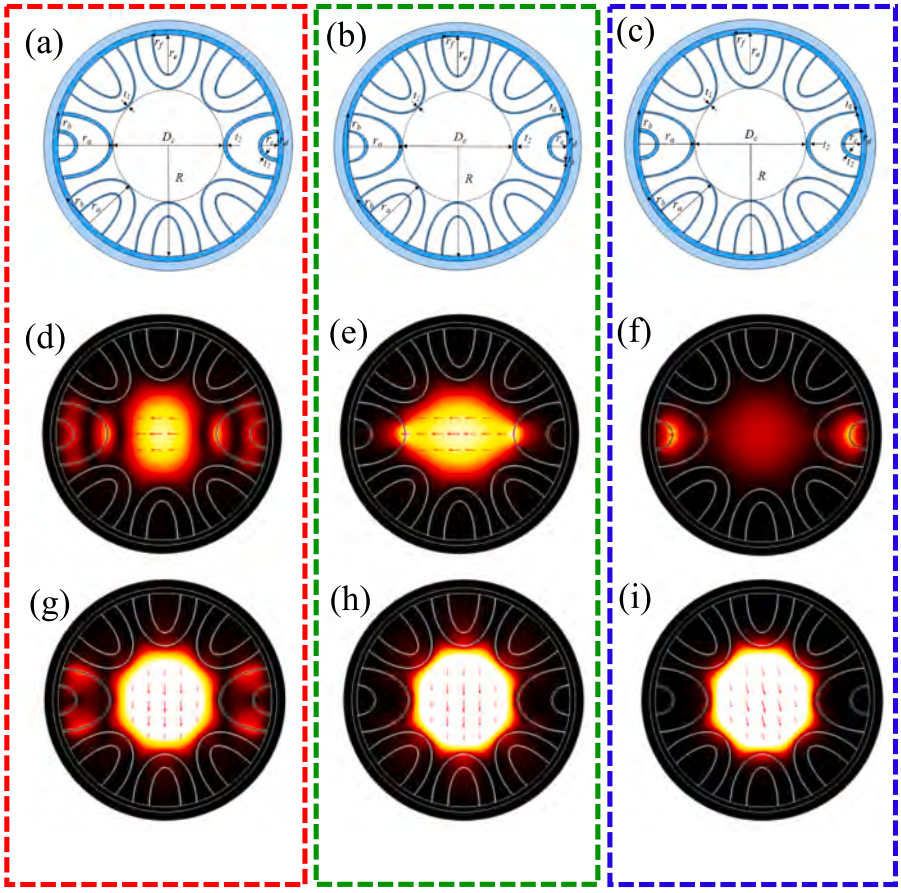

Fig. 2. Cross-sections of HC-ARF with different nesting structures and mode field diagrams of X-polarized FM and Y-polarized FM at 1 THz.

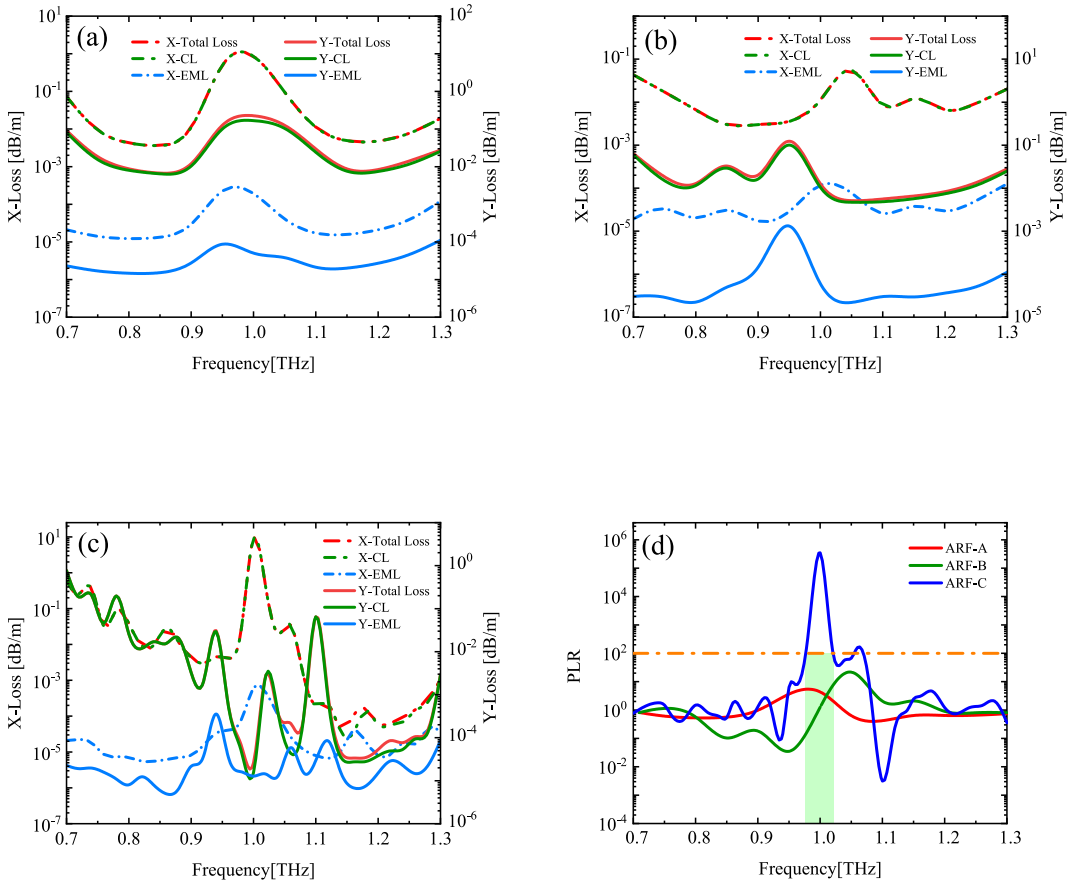

Fig. 3. CL, EML, and total loss of three double-layer nested structures: (a) ARF-A, (b) ARF-B, (c) ARF-C, and (d) PLR.

uniform wall thickness in the inner layer enhance the loss of X-polarized FM and reduce the loss of Y-polarized FM. The maximum thickness of the outer semi-elliptical tube is $t_2 = 0.1$ mm, the minimum wall thickness is $t_0 = 0.039$ mm, the major axis $r_a = 3.05$ mm, and the ellipticity $u = r_b/r_a = 0.61$. The wall thickness of the inner semi-elliptical tube is $t_2 = 0.1$ mm, the major axis $r_c = 1.1$ mm, and the ellipticity $v = r_d/r_c = 0.8$. In the Y-axis direction, the six double-layer nested semi-elliptic tubes with a uniform wall thickness are adopted. The major and minor axes of the outer elliptical tubes are the same as those of the X-axis elliptical tubes, and the wall thickness is $t_1 = 0.035$ mm. The major axis of the inner elliptic tube is $r_e = 2.3$ mm and the ellipticity $w = r_f/r_e = 0.4$. The thickness of the jacket tube and the perfectly matched layer are $JT = 0.3$ mm and $T = 0.5$ mm, the core diameter is $D_c = 6.2$ mm, and the inner radius of the jacket tube is $R = 6.15$ mm.

3. Results and discussion

According to the basic principle of HC-ARF, the fiber core mode at the resonant frequency will generate high transmission loss, while the fiber core mode in the anti-resonant frequency region transmits with low loss. The resonant frequency and anti-resonant frequency can be calculated by Eq (1) [26–28]:

$$f_c = \frac{mc}{2t\sqrt{n^2-1}} \tag{1}$$

where c is the speed of light in vacuum, m is the resonance order, n is the refractive index of the HRS material, which is 3.417 in the range between 0.5 and 4.5 THz [29], and t is the wall thickness of the cladding tube. The initial parameters of the structure are calculated by inputting $f_c = 1$THz, $m = 1$ and 2 into formula (1). The resonant wall thicknesses are 0.045 mm and 0.09 mm respectively. In order to control the Y-polarized FM in the anti-resonant region, the wall thickness of the Y-axis should avoid above values. By continuous optimizing the wall thicknesses $t_1 = 0.035$ mm of the Y-axis is chosen as the optimal value. Meanwhile X-polarized FM should satisfy the resonant condition, the wall thicknesses of the X-axis should be near 0.045 mm or 0.09 mm. Finally the loss of the X-polarized FM reaches maximum as $t_2 = 0.1$ mm, the corresponding resonant frequencies is 0.92 THz.

The transmission loss of ARF includes the confinement loss (CL) and effective material loss (EML), as shown in Eqs. (2) and (3), respectively [30,31]:

$$\mathrm{CL} = 8.686\left(\frac{2\pi f}{c}\right)\mathrm{Im}\left(n_{eff}\right), [\mathrm{dB/m}] \tag{2}$$

$$\mathrm{EML} = 4.34\sqrt{\frac{\varepsilon_0}{\mu_0}}\frac{\int_{A_{mat}} n\alpha_{mat}|E|^2 dA}{2\int_{All} S_z dA}, [\mathrm{dB/m}] \tag{3}$$

where f is the operating frequency, Im (n_{eff}) is the imaginary part of the effective refractive index, and ε_0 and μ_0 are the permittivity and permeability in vacuum, respectively. α_{mat} is the absorption coefficient of the HRS and less than 0.015c m^{-1} in the range of 0.1–1.5 THz[32], and S_z is the Poynting vector along the z-direction.

The PLR of a single polarized fiber is defined as the loss ratio of the X-polarized FM to the Y-polarized FM as shown by Eq. (4):

$$\mathrm{PLR} = X_{Loss}/Y_{Loss}. \tag{4}$$

Three double-layer nested semi-elliptical tube structures with a uniform wall thickness (ARF-A), asymptotic wall thickness (ARF-B), and mixed uniform and asymptotic wall thickness (ARF-C) are analyzed, as shown in Fig. 2(a), (b), and (c). The corresponding mode field

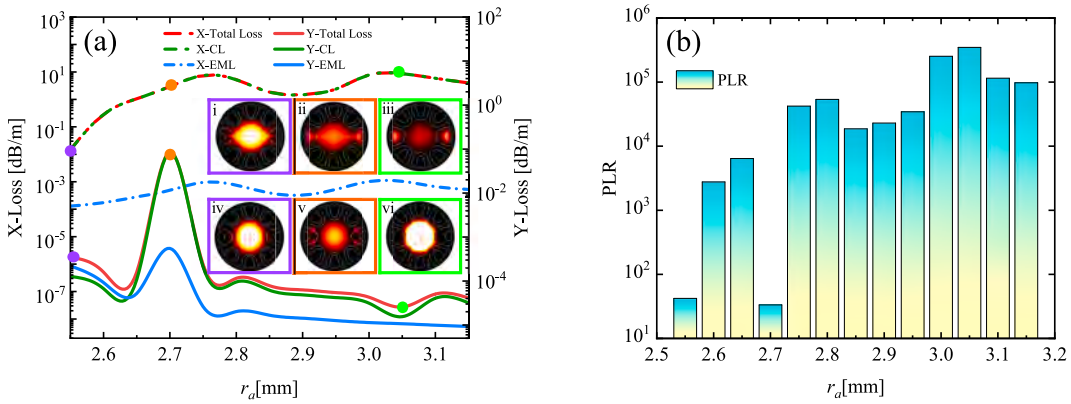

Fig. 4. (a) CL, EML, and total loss and (b) PLR for different r_a at 1 THz.

distributions of X-polarized and Y-polarized FMs at 1 THz are also shown. The uniform semi-elliptical tubes of ARF-A with a wall thickness $t_2 = 0.1$ mm cause the X-polarized FM to couple to the outer and inner cladding tube, as shown in Fig. 2(d). It increases the X-polarized FM transmission loss because the wall thickness is near the resonant frequency at 1THz.It produces Y-polarized FM coupling to the cladding, although the wall thickness of the six double-layer nested semi-elliptic tubes in the Y-axis direction is $t_1 = 0.035$ mm, which corresponds to the anti-resonance region. Therefore, the Y-polarized FM also generates losses, and the ARF-A structure shows a lower PLR.

Fig. 3(a) shows the CL, EML, and total loss of the structure in the range of 0.7–1.3 THz. The EMLs of both X- and Y-polarized FMs are lower than CLs due to the small material absorption coefficient of the HRS. Therefore, CLs play a major role in the total loss. The CLs of the X-polarized and Y-polarized FMs increase near 1 THz due to the resonance effect of the X-axis cladding tube, and the PLR is smaller, as shown by the red solid line in Fig. 3(d). It means that a simple double-layer nested cladding tube with a uniform wall thickness in the X-axis direction cannot effectively enhance PLR. The double-layer nested semi-elliptical tube structure with gradual wall thicknesses is analyzed, as shown in Fig. 2(b). The maximum wall thickness of the outer and inner layers of the two nested cladding tubes in the X axis is $t_2 = 0.1$ mm, while the minimum wall thicknesses are $t_0 = 0.039$ mm and $t_3 = 0.035$ mm, respectively. Since the gradual wall thickness changes the resonance conditions of the X-polarized and Y-polarized FMs, the mode fields of the X-polarized and Y-polarized FMs are better confined in the fiber core at 1 THz, as shown in Fig. 2(e) and (h). Compared with the ARF-A structure, the transmission loss of the ARF-B structure decreases overall, and the resonant frequency region shifts, as shown in Fig. 3(b). The PRL is shown by the green solid line in Fig. 3(d), the PLR is not better near 1 THz.

The hybrid double-layer nested structure with gradual wall thickness of the outer layer and uniform wall thickness of the inner layer is shown in Fig. 2(c). Since the wall thickness of the inner cladding tube satisfies the resonance condition and the X-polarized FM is strongly coupled to the cladding, as shown in Fig. 2(f), the loss increases significantly compared to ARF-A and ARF-B. Meanwhile, the gradual wall thickness of the outer cladding tube confines the Y-polarized FM in the core region, as shown in Fig. 2 (i). Fig. 3(c) shows the loss spectra of ARF-C in the range of 0.7–1.3 THz. Compared with ARF-A and ARF-B, the EML changes less. The total loss of X-polarized FM increases significantly, and the maximum of 9.07 dB/m appears at 1 THz. At the same time, the total loss of the Y-polarized FM is only 2.59×10^{-5} dB/m near 1 THz. Fig. 3 (d) shows that the maximum PLR near 1 THz is 349,318. The PLR values are bigger than 100 in the range between 0.98 and 1.02 THz indicating excellent single polarization properties.

The effects of the major axis r_a of the outer cladding semi-elliptical tube on the PLR are investigated. Fig. 4(a) shows the loss spectra when r_a is 2.50–3.15 mm. When $r_a = 2.5$ mm, the outer layer tube with the resonant wall thickness plays a major role in coupling the X-polarized FM with the outer layer tube, as shown in the inset i in Fig. 4(a). With increasing r_a, the distance between the outer and inner cladding tubes increases, causing the X-polarized FM to couple to the uniform-wall-thickness inner cladding tube, as shown in inset ii of Fig. 4(a), which reveals an increase in CL. When r_a is increased to 3.05 mm, the X-polarized FM is further coupled to the cladding, as shown in inset iii in Fig. 4(a), and CL further increases to 9.07 dB/m. Meanwhile, r_a also affects the loss of Y-polarized FM. When $r_a = 2.5$ mm, inset iv in Fig. 4(a) shows that a small portion of the Y-polarized FM couples to the outer cladding tube, but only produces a small loss. When r_a gradually increases, the Y-polarized FM is gradually coupled to the outer cladding tube, as shown in inset v in Fig. 4(a), and the loss peak appears at $r_a =$ 2.7 mm. However, the Y-polarized FM is no longer affected upon further

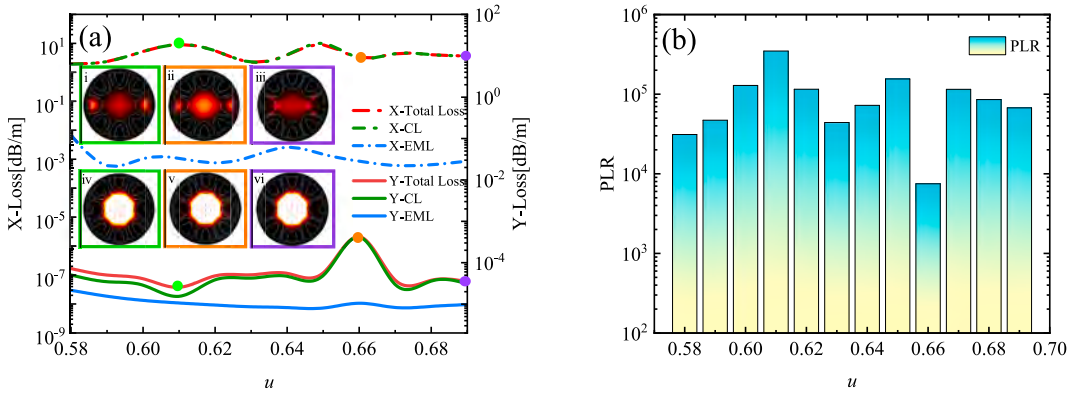

Fig. 5. (a) CL, EML, and total loss and (b) PLR for different ellipticity u at 1 THz.

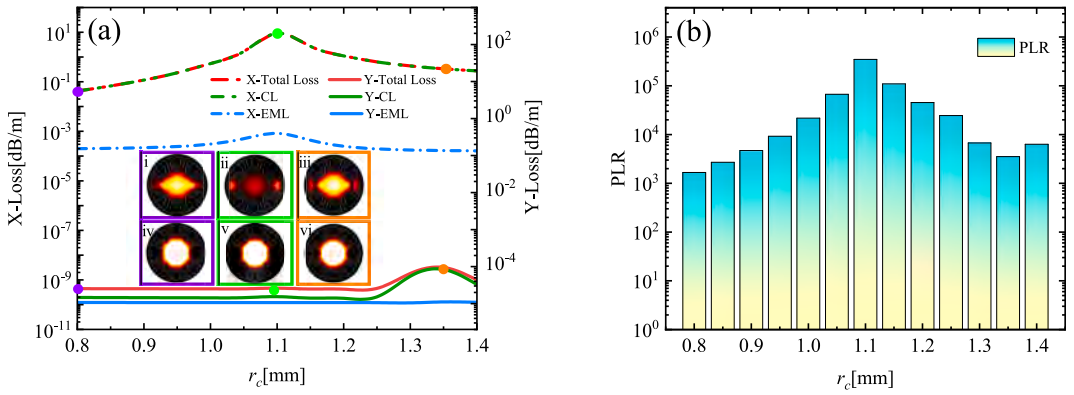

Fig. 6. (a) CL, EML, and total loss and (b) PLR for different r_c at 1 THz.

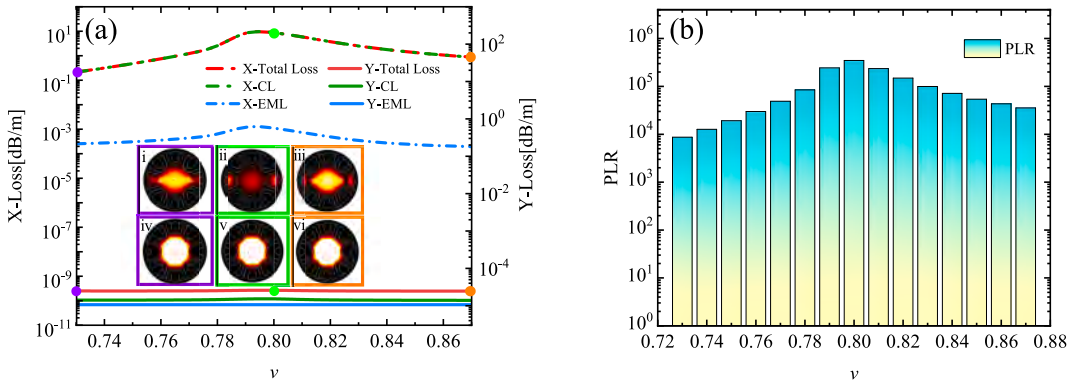

Fig. 7. (a) CL, EML, and total loss and (b) PLR for different ellipticity v at 1 THz.

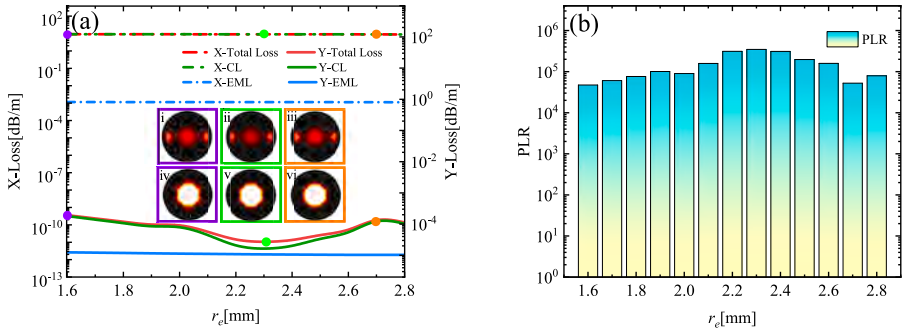

Fig. 8. (a) CL, EML, and total loss and (b) PLR for different r_e at 1 THz.

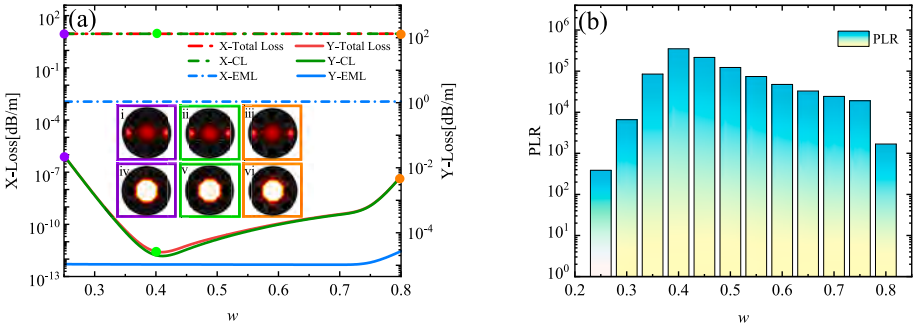

Fig. 8. (a) CL, EML, and total loss and (b) PLR for different r_e at 1 THz.

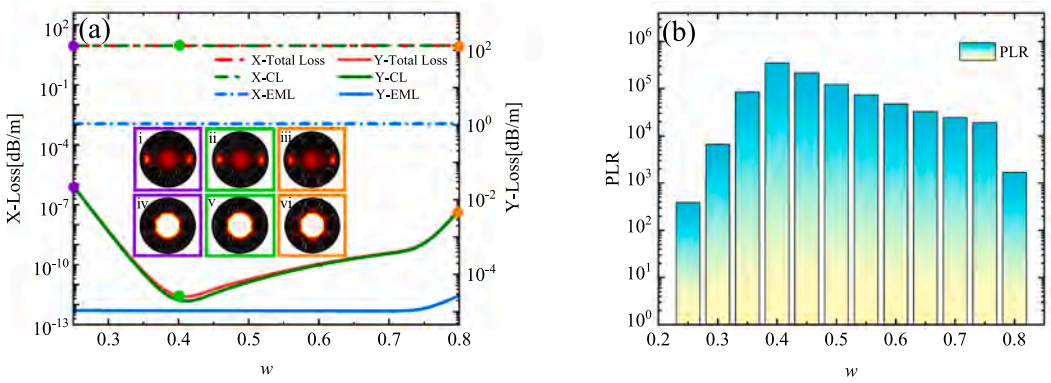

Fig. 9. (a) CL, EML, and total loss and (b) PLR for different ellipticity w at 1 THz.

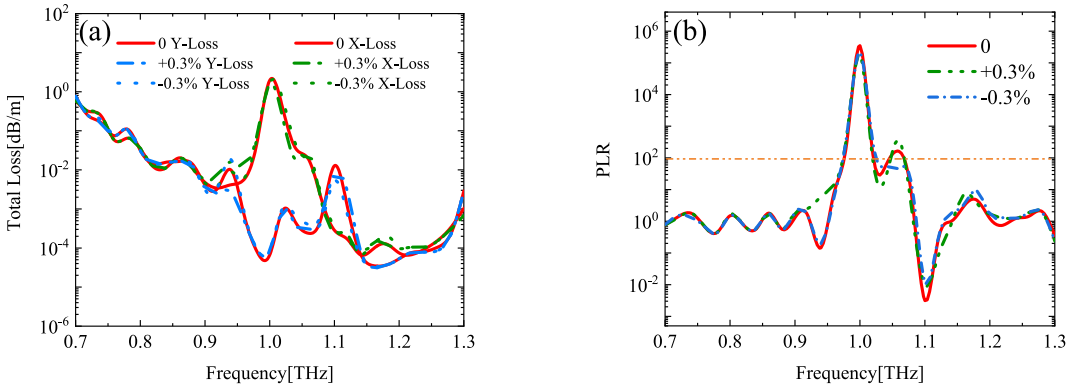

Fig. 10. (a) Effect of the thickness t_2 on the total loss and (b) PLR.

increasing r_a and is rather confined in the fiber core region, as shown in inset vi in Fig. 4(a). The Y-polarized FM loss is the smallest of 2.59×10^{-5} dB/m at $r_a = 3.05$ mm. The maximum PLR is 349,318 as shown in Fig. 4(b). Therefore, $r_a = 3.05$ mm is selected as the optimal value.

The influence of the ellipticity u of the cladding tube on the PLR is studied. The loss spectra are shown in Fig. 5(a) for u being 0.58–0.69. The X-polarized FM is coupled to the cladding, as shown in insets i, ii, and iii in Fig. 5(a), resulting in larger CL. However, the variation of loss is smaller. The Y-polarized FM is better bound within the fiber core, as shown in insets iv, v, and vi in Fig. 5(a). A small portion of the Y-polarized FM couples to the outer cladding tube when u is about 0.66, giving rise to a slightly larger loss. This indicates that the ellipticity u in the range of 0.58–0.69 has a smaller influence on X-polarized and Y-polarized losses, and PLR changes slightly, as shown in Fig. 5(b). The best PLR corresponds to $u = 0.61$.

The effects of the major axis r_c of the inner semi-elliptical tube nested on the X-polarized and Y-polarized FM losses are shown in Fig. 6(a). When r_c is between 0.8 and 1.4 mm, the total loss of the X-polarized FM increases initially and then decreases. This is because the spacing between the inner nested tubes and the outer nested tubes determines the coupling between the core mode and the cladding mode. The strongest coupling appears at $r_c = 1.1$ mm, as shown in insets i, ii, and iii in Fig. 6 (a). Meanwhile, r_c has smaller effects on the Y-polarized FM. The Y-polarized FM is better confined in the core region as shown in insets iv, v, and vi in Fig. 6 (a). Fig. 6(b) shows that the largest PLR is observed at $r_c = 1.1$ mm. Subsequently, the effects of the ellipticity v is analyzed, as shown in Fig. 7(a). The ellipticity v has no effect on the loss of the Y-polarized FM, and only affects the coupling of the X-polarized FM to the

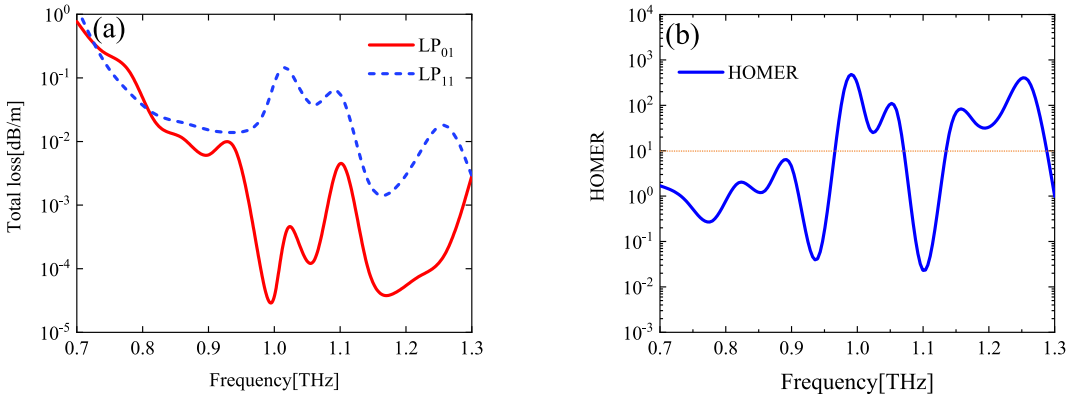

Fig. 11. (a) The total losses of the Y-polarized LP_{01} and LP_{11} and (b) HOMER.

Table 1
Properties of single-polarization HC-ARFs.

References	Frequency [THz]	X-Loss [dB/m]	Y-Loss [dB/m]	PLR
[22]	0.9	12	4.8	2.5
[23]	1.1	4.42	0.34	13
[24]	0.5	153	0.98	156
[25]	1	1802	1.18	1527
Our work	1	9.07	2.59×10^{-5}	349,318

cladding mode. The PLR reaches the maximum when $v = 0.8$.

The effects of the major axis r_e and ellipticity w of the six inner nested semi-elliptical tubes in the Y-axis direction on the PLR are investigated. Fig. 8(a) shows the loss spectra for r_e between 1.6 and 2.8 mm, and r_e hardly affects the loss of the X-polarized FM, while the total loss remains constant. However, it affects the loss of Y-polarized FM, which can further reduce the loss of Y-polarized FM, resulting in a large fluctuation of the Y-polarized FM loss. The strongest constraint on the Y-polarized FM is obtained at $r_e = 2.3$ mm, which corresponds to the largest PLR, as shown in Fig. 8(b). Therefore, $r_e = 2.3$ mm is selected as the optimal value. The effects of ellipticity w on the X-polarized and Y-polarized FMs are shown in Fig. 9(a). It only influences the loss of Y-polarized FM in the range of 0.25–0.8. The CL of the Y-polarized FM decreases first and then increases. As shown in insets iv, v, and vi in Fig. 9(a), a larger or smaller w leads to a leakage of the mode field. A proper ellipticity can better limit the Y-polarized FM. The total loss of Y-polarized FM reaches the minimum, and the PLR is maximum for $w = 0.4$, as shown in Fig. 9(b).

In the actual processing process the fabrication error of the HC-ARF is unavoidable, therefore the fabrication tolerance is discussed. The wall thickness of the cladding tube is the key factor. Fig. 10 (a) compares the change of total loss as t_2 changes ± 3 %. It can be seen that the ± 0.3 % change of the wall thickness has little effect on the loss of X-polarized FM and Y-polarized FM. At 1THz the PLR slightly reduce but still maintain a higher value, as shown in Fig. 10(b). The result shows that the designed HC-ARF can reach the fabrication tolerances.

Higher order mode extinction ratio (HOMER) is commonly employed to assess the single-mode performance of HC-ARFs. A fiber with a HOMER value exceeding 10 can effectively operate as a single-mode fiber [33]. The Y-polarized losses of the LP11 and LP01 modes are calculated and compared as shown in Fig. 11(a). The loss of the HOM LP11 is significantly greater than that of LP01 mode. Meanwhile, the HOMER is also calculated as shown in Fig. 11(b). In the range of 0.98–1 THz the HOMER are greater than 10. It means that the HOM will leakage and has little influence on the FM. The designed HC-ARF can maintain single-mode transmission.

Table 1 compares the properties of recently reported single-polarization HC-ARFs for the terahertz band. It can be seen that the transmission loss of the Y-polarized FM of our HC-ARF is much lower than the previous reported results. The lowest Y-polarized transmission loss of 2.59×10^{-5} dB/m and the X-polarized transmission loss of 9.07 dB/m mean that the designed HC-ARF can be adopted to design single-polarization fiber. Meanwhile the ultra-high PLR of 349,318 at 1 THz exhibits excellent polarization filtering performance and has great application prospects.

4. Conclusion

A single-polarization HC-ARF with ultra-low loss and ultra-high PLR is designed and analyzed. The HC-ARF adopts a double-layer nested semi-elliptic tube structure. In the X-axis direction, the outer and inner layer tubes have gradually changing wall thicknesses and a uniform wall thickness, respectively. The structure increases the loss of the X-polarized FM but reduces the loss of the Y-polarized FM. At 1 THz, the losses of X-polarized FM and Y-polarized FM are 9.07 dB/m and 2.59×10^{-5} dB/m, respectively. The PLR is as large as 349,318, and it is greater than 100 in the range between 0.98 and 1.02 THz. The properties of the HC-ARF are much better than those of similar filters reported recently boding well for many THz applications. Meanwhile, the design concept of the gradually changing wall thicknesses provides a new method to study different types of HC-ARF. Although the novel structure brings a challenge to the fabrication of HC-ARF, it is believed that the similar HC-ARF can be achieved with the development of the optical fiber manufacturing technology and applies in the fields of communication and sensing.

CRediT authorship contribution statement

Qiang Liu: Writing – review & editing, Writing – original draft, Supervision, Software, Project administration, Methodology, Investigation. **Xiaotian Yao:** Writing – original draft, Software, Methodology, Investigation, Funding acquisition, Formal analysis, Data curation, Conceptualization. **Jian Han:** Resources. **Guangrong Sun:** Software, Investigation. **Zihao Lan:** Software. **Peiqing Xing:** Software. **Jingwei Lv:** Software, Resources. **Paul K. Chu:** Writing – review & editing, Software, Resources. **Chao Liu:** Software.

Declaration of competing interest

The authors declare that they have no known competing financial interests or personal relationships that could have appeared to influence the work reported in this paper.

Acknowledgments

This work was jointly supported by the Basic Research Support Project for the Excellent Youth Scholars of Heilongjiang Province [YQJH2023077], Hainan Province Science and Technology Special Fund [ZDYF2022GXJS222], Natural Science Foundation of China [12304480], Heilongjiang Provincial Natural Science Foundation of China [JQ2023F001], Local Universities Reformation and Development Personnel Training Supporting Project from Central Authorities, Natural Science Foundation of Heilongjiang Province [LH2021F007], China Postdoctoral Science Foundation funded project [2020 M670881], City University of Hong Kong Strategic Research Grant (SRG) [7005505], as well as City University of Hong Kong Donation Research Grant [DON-RMG 9229021].

Data availability

The data that has been used is confidential.

References

[1] H. Hu, W. Lin, X. Ma, et al., Terahertz 3-D fast line-scanning imaging using 3-D printed devices, Opt. Express 32 (3) (2024) 4111.
[2] L. Liang, X. Hu, L. Wen, et al., Unity integration of grating slot waveguide and microfluid for terahertz sensing, Laser Photonics Rev. 12 (11) (2018) 1800078.
[3] J. Dong, A. Tomasino, G. Balistreri, et al., Versatile metal-wire waveguides for broadband terahertz signal processing and multiplexing, Nat. Commun. 13 (741) (2022) 1–8.
[4] J. Ma, R. Shrestha, J. Adelberg, et al., Security and eavesdropping in terahertz wireless links, Nature 563 (2018) 89–93.
[5] P. Huang, Y. Cao, J. Chen, et al., Analysis and inspection techniques for mouse liver injury based on terahertz spectroscopy, Opt. Express 27 (18) (2019) 26014.
[6] M. Nagel, P. Bolivar, M. Brucherseifer, et al., Integrated THz technology for label-free genetic diagnostics, Appl. Phys. Lett. 80 (1) (2002) 154.
[7] X. Lu, L. Sun, P. Jiang, et al., Progress of photodetectors based on the photothermoelectric effect, Adv. Mater. 31 (50) (2019) 1902044.
[8] D. Wu, F. Yu, Y. Liu, et al., Dependence of waveguide properties of anti-resonant hollow-core fiber on refractive index of cladding material, J. Lightwave Technol. 37 (21) (2019) 5593–5599.
[9] A. Sufian, E. Baleine, J. Geldmeier, et al., Light transmission through a hollow core fiber bundle, IEEE J. Sel. Top. Quantum Electron. 30 (6) (2024) 4301308.
[10] G. Humbert, J.C. Knight, G. Bouwmans, et al., Hollow core photonic crystal fibers for beam delivery, Opt. Express 12 (8) (2004) 1477–1484.
[11] Y. Wang, W. Chang, Multi-nested antiresonant hollow-core fiber with ultralow loss and single-mode guidance, Opt. Express 31 (11) (2023) 18250–18264.

[12] S. Zhao, Q. Liu, Y. Liu, et al., Navigation-grade resonant fiber-optic gyroscope using ultra-simple white-light multibeam interferometry, Photonics Res. 10 (2) (2022) 542–549.
[13] M. Ivanov, É. Doiron, M. Scaglia, et al., Advancing high-power hollow-core fiber pulse compression, IEEE J. Sel. Top. Quantum Electron. 30 (6) (2024) 5100310.
[14] F. Gérôme, K. Cook, A.K. George, et al., Delivery of sub-100fs pulses through 8m of hollow-core fiber using soliton compression, Opt. Express 15 (12) (2007) 7126–7131.
[15] M. Ueffing, S. Reiger, M. Kaumanns, et al., Nonlinear pulse compression in a gas-filled multipass cell, Opt. Lett. 43 (9) (2018) 2070–2073.
[16] X. Zhao, J. Xiang, X. Wu, et al., High birefringence, single-polarization, low loss hollow-core anti-resonant fibers, Opt. Express 29 (22) (2021) 36273–36286.
[17] R. Yao, Y. Xiao, Y. Lai, Design of a negative curvature hollow-core fiber for transmitting a single-mode dark hollow beam, Optik 288 (2023) 171147.
[18] H. Chen, H. Wang, H. Hou, et al., A terahertz single-polarization single-mode photonic crystal fiber with a rectangular array of micro-holes in the core region, Opt. Commun. 285 (2012) 3726–3729.
[19] S. Yan, S. Lou, W. Zhang, et al., Single-polarization single-mode double-ring hollow-core anti-resonant fiber, Opt. Express 26 (24) (2018) 31160–31171.
[20] S. Yan, Z. Lian, S. Lou, et al., Single-polarization single-mode hollow-core negative-curvature fiber with silicon-coated cladding, Opt. Quant. Electron. 52 (5) (2020) 1–12.
[21] Y. Gong, Y. Meng, Single-polarization single-mode broadband ultra-low loss hollow-core anti-resonant fiber with nested double C-type cladding tubes, Opt. Commun. 552 (2024) 130062.
[22] I.M. Ankan, M.A. Mollah, A.K. Paul, et al., Polarization-maintaining and polarization-filtering negative curvature hollow core fiber in THz regime, IEEE Tensymp 612–615 (2020).
[23] M.A. Mollah, S. Rana, H. Subbaraman, Polarization filter realization using low-loss hollow-core anti-resonant fiber in THz regime, Results Phys. 17 (2020) 103092.
[24] L. Xue, X. Sheng, H. Jia, et al., Single-polarization low loss terahertz hollow-core anti-resonant fiber with high polarization loss ratio, Opt. Commun. 537 (2023) 129460.
[25] Q. Liu, G. Sun, Y. Sun, et al., High-performance terahertz polarization filter based on the anti-resonant fiber, Optik 288 (2023) 171247.
[26] Y. Hong, S. Gao, W. Ding, et al., Highly birefringent anti-resonant hollow-core fiber with a bi-thickness fourfold semi-tube structure, Laser Photonics Rev. 16 (2022) 2100365.
[27] Y. Wu, M. Chen, Z. Dai, Review on the terahertz transmission devices and their applications: from metal waveguides to terahertz fibers, Opt. Laser Technol. 183 (2025) 112339.
[28] C.-H. Lai, Y.-S. Yeh, C.-A. Yeh, et al., Effective bandwidth of terahertz antiresonant reflecting pipe waveguide, Opt. Express 26 (5) (2018) 6456–6465.
[29] G. Sun, Q. Liu, H. Mu, et al., Anti-resonant fiber with nested U-shape tubes for low-loss terahertz waveguides, Opt. Laser Technol. 163 (2023) 109424.
[30] Q. Liu, K. Wang, Y. Sun, et al., Surface plasmon resonance methane sensor based on the D-type photonic quasi-crystal fiber with double-layer films, Opt. Fiber Technol. 84 (2024) 103779.
[31] Q. Liu, G. Sun, H. Mu, et al., Hybrid nested negative curvature fiber with ultra-low-loss in the terahertz band, Infrared Phys. Technol. 136 (2024) 105003.
[32] J. Dai, J. Zhang, W. Zhang, et al., Terahertz time-domain spectroscopy characterization of the far-infrared absorption and index of refraction of high-resistivity, float-zone silicon, Opt. Soc. Am. b. 21 (7) (2004) 1379–1386.
[33] K.S.R. Shaha, A. Khaleque, M.S. Hosen, Wideband low loss hollow core fiber with nested hybrid cladding elements, J. Lightwave Technol. 39 (20) (2021) 6585–6591.